Contents lists available at ScienceDirect

Translational Oncology

Original Research

Anti-tumor effect of carrimycin on oral squamous cell carcinoma cells *in vitro* and *in vivo*

Si-yuan Liang[1], Tong-chao Zhao[1], Zhi-hang Zhou[1], Wu-tong Ju, Ying Liu, Yi-ran Tan, Dong-wang Zhu, Zhi-yuan Zhang, Lai-ping Zhong*

Department of Oral and Maxillofacial-Head and Neck Oncology, Ninth People's Hospital, College of Stomatology, Shanghai Jiao Tong University School of Medicine; National Clinical Research Center for Oral Diseases; Shanghai Key Laboratory of Stomatology, No. 639 Zhizaoju Road, Shanghai 200011, China

ARTICLE INFO

ABSTRACT

Purpose: : Carrimycin is a newly synthesized macrolide antibiotic with good antibacterial effect. Exploratory experiments found its function in regulating cell physiology, proliferation and immunity, suggesting its potential anti-tumor capacity. The aim of this study is to investigate the anti-tumor effect of carrimycin against human oral squamous cell carcinoma cells *in vitro* and *in vivo*.

Methods: : Human oral squamous cell carcinoma cells (HN30/HN6/Cal27/HB96 cell lines) were treated with gradient concentration of carrimycin. Cell proliferation, colony formation and migration ability were analyzed. Cell cycle and apoptosis were assessed by flow cytometry. The effect of carrimycin on OSCC *in vivo* was investigated in tumor xenograft models. Immunohistochemistry, western blot assay and TUNEL assays of tissue samples from xenografts were performed. The key proteins in PI3K/AKT/mTOR pathway and MAPK pathway were examined by western blot.

Results: : As the concentration of carrimycin increased, the proliferation, colony formation and migration ability of OSCC cells were inhibited. After treating with carrimycin, cell cycle was arrested in G0/G1 phase and cell apoptosis was promoted. The tumor growth of xenografts was significantly suppressed. Furthermore, the expression of p-PI3K, p-AKT, p-mTOR, p-S6K, p-4EBP1, p-ERK and p-p38 were down-regulated *in vitro* and *in vivo*.

Conclusions: : Carrimycin can inhibit the biological activities of OSCC cells *in vitro* and *in vivo*, and regulate the PI3K/AKT/mTOR and MAPK pathways.

Introduction

Oral squamous cell carcinoma (OSCC) is one of the most common malignant tumors in the oral and maxillofacial region, with a high tendency of local invasion and lymph node metastasis. Currently, the main treatment is the combined sequence therapy based on surgery. Despite progress achieved in diagnostic and therapeutic strategies, the overall prognosis of the OSCC patients is poor, with the 5-year survival rate of only 50%–60% [1, 2]. Chemotherapy is an important part of the combined sequence therapy, the recommended first-line drug for advanced head and neck cancer is primarily cisplatin, with other agents reserved mainly for patients who may not tolerate cisplatin. However, the clinical application of chemotherapy does not always achieve satisfactory results. The reasons include the toxic and side effects of traditional chemotherapy drugs and drug resistance of tumors.

Traditional chemotherapy drugs include alkylating agent, antimetabolic drugs, hormone drugs, platinum drugs, botanical drugs, an-

tibiotic drugs, molecular-targeted drugs, and so on, which are usually combined to exert anti-tumor effect. Because of malnutrition, immune barrier breakdown induced by radiotherapy and chemotherapy, and ischemic necrosis in tumor center, patients with malignant tumor are more likely to be involved in perioperative infection. Thus, antibiotic drugs may play a dual role in anti-infection and anti-tumor functions, indicating its importance in cancer treatment. However, there are also apparent systemic toxicities of current anti-tumor antibiotics, for example, cardiotoxicity and bone marrow suppression of anthracycline drugs, pulmonary fibrosis induced by bleomycin and cytotoxicity of human erythrocyte caused by macrolides [3-5]. Thus, there is an urgent need of finding new drugs with both good anti-tumor activity and low biotoxicity.

Carrimycin (trade name: Bite, formerly shengjimycin and bitespiramycin), a new genetic engineering 16-membered macrolide antibiotic, is a mixture of isovalerylspiramycin I, II and III, and a certain amount of (iso)butyryl/propionyl/acetylspiramycin III and(iso)butyryl/propionyl/acetylspiramycin II (Fig. 1a) [6]. Completed

---

* Corresponding author.
  E-mail address: zhonglp@hotmail.com (L.-p. Zhong).
[1] These authors contributed equally to this work.

A

Isovalerylspiramycins III R=COCH$_2$CH$_3$ R'=COCH$_2$CH(CH$_3$)$_2$
Isovalerylspiramycins II   R=COCH$_3$ R'=COCH$_2$CH(CH$_3$)$_2$
Isovalerylspiramycins I   R=H   R'=COCH$_2$CH(CH$_3$)$_2$
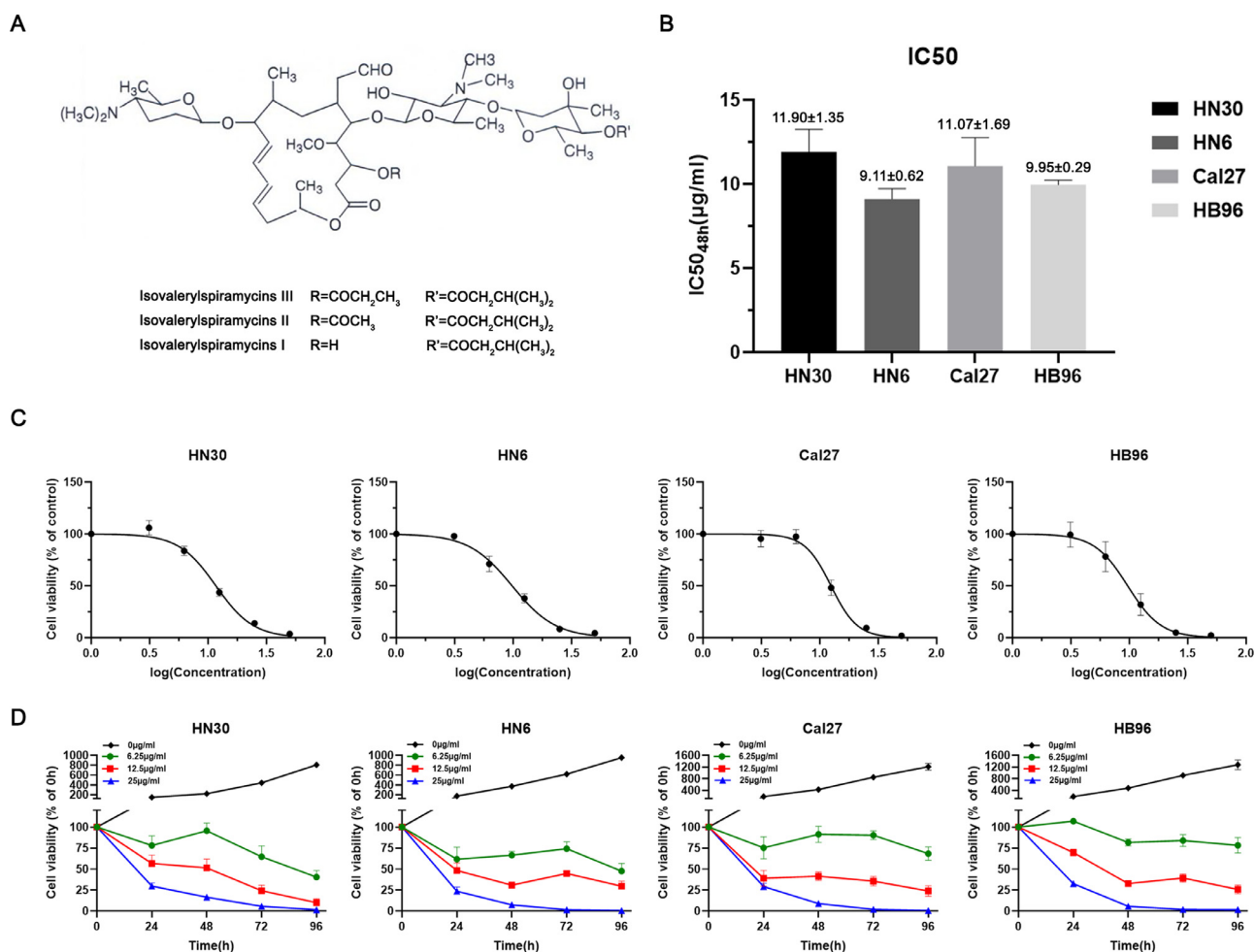
B

C

D

Fig. 1. A) The structure of the mainly ingredients of carrimycin6. (B-D) the effect of carrimycin on cell viability was measured by the Cell Counting Kit-8 assay. The growth of HN30,HN6,Cal27 and HB96 cells treated with carrimycin was inhibited in a time and dose dependent manner, and the IC50(48 h) was shown. All experiments were performed three times.

phase III clinical trial showed an excellent anti-bacterial effect of carrimycin, as well as good bioavailability and high biosafety. Further investigation found that carrimycin not only acted as an antibiotic but also regulated cell physiology, proliferation and other activities, suggesting its potential role on tumor suppression. However, the specific mechanism remained unclear.

In this study, the anti-tumor effect of carrimycin on OSCC was investigated *in vitro* and *in vivo* for the first time. Moreover, we preliminarily explored the molecular mechanism, aiming to provide scientific basis and experimental data for achieving the clinical application of carrimycin in OSCC.

Materials and methods

Cell culture

Four OSCC cell lines of HN30, HN6, Cal27 and HB96 were used in this study. HN30 and HN6 were from the National Institutes of Health of the United States of America. Cal27 was purchased from American Type Culture Collection (ATCC) (Manassas, USA). HB96 was from our previously established *in vitro* cellular carcinogenesis model of OSCC [7, 8]. All cells were cultured in Dulbecco's modified Eagle medium (DMEM) (Gibco, USA) supplemented with 10% fetal bovine serum (FBS) and maintained in a humidified atmosphere with 5% CO$_2$ at 37 °C. Cell lines were authenticated every six month and regularly tested for bacterial contamination or mycoplasma infection.

Cell viability assay

The effect of carrimycin on cell viability was measured by the Cell Counting Kit-8 assay (CCK-8, Dojindo Laboratories, Japan) according to the manufacturer's protocol. Cells were seeded in triplicate in 96-well plates at a density of 1.6×10^3/well, and treated with carrimycin at a concentration gradient of 50 μg/ml, 25 μg/ml, 12.5 μg/ml, 6.25 μg/ml, 3.125 μg/ml and 0 μg/ml. After culturing for 24–96 h, cells were incubated with CCK-8 reagents (10μl/well) at 37 °C for 2 h. The absorbance at 450 nm was measured by the enzyme-linked immunosorbent assay reader(Molecular Devices, USA).

Colony formation assay

Cells were seeded in 6-well plates at a density of 8×10^2/well and treated with carrimycin at a concentration gradient of 10 μg/ml, 5 μg/ml and 0 μg/ml. After culturing at 37 °C with 5% CO$_2$ for 2 weeks, during which fresh medium was changed every three days, the cell colonies were fixed by 4% paraformaldehyde for 30 min, followed by staining with 0.5% crystal violet solution. Colonies with more than 50 cells were counted.

Wound-healing assay

Cells were seeded in 6-well plates and incubated at 37 °C with 5% CO$_2$ until the bottom of the well was completely covered by a monolayer

of cells. After 12 h starvation in FBS-free DMEM, 10 μg/ml or 0 μg/ml carrimycin (diluted with 3%FBS DMEM) were added and wounds were made using a 10-μl pipette tip. Photographs of wound closure at 0 h and 15 h were captured.

Cell cycle analysis

The cell cycle was labeled using cell cycle detection kit (Signalway Antibody, USA) and analyzed by flow cytometry. Cells were starved in FBS-free DMEM for 12 h, followed by treating with carrimycin at a concentration of 10 μg/ml and 0 μg/ml at 37 °C with 5% CO_2 for 24 h. Cells were harvested and fixed with 70% cold ethanol for 2 h. 20μl RNAse was added into each tube and incubated at 37 °C for 30 min. Intracellular DNA was labeled with propidium iodide (PI) at 4 °C for 30 min. The samples were assayed by flow cytometer (FACSCalibur^{TM}, BD Biosciences, San Jose, CA, USA). The results were analyzed by ModFit LT^{TM} software (BD Biosciences).

Apoptosis assay by flow cytometry

Cell apoptosis was analyzed by flow cytometry. Cells were treated with carrimycin at a concentration gradient of 10 μg/ml, 5 μg/ml and 0 μg/ml at 37 °C with 5% CO_2 for 24 h, and harvested for double-staining with the FITC-Annexin V Apoptosis Detection Kit (BD Biosciences, Franklin Lakes, NJ, USA) according to the manufacturer's instructions. The samples were assayed by flow cytometer (FACSCalibur^{TM}, BD Biosciences, San Jose, CA, USA). The results were analyzed by FlowJo software (BD Biosciences).

Western blot assay

Cells treated with carrimycin at 0 μg/ml, 5 μg/ml, 10 μg/ml for 24 h were lysed in RIPA assay buffer (Sigma-Aldrich, St Louis, MO, USA) and protein concentrations were determined using a bicinchoninic acid assay (Abcam, USA). Protein lysates (20 μg/lane) were separated by SDS-PAGE (6–12% gels) and then transferred onto PVDF membranes using a semidry transfer system (Bio-Rad, USA). The membranes were blocked in 5% skim milk (Becton Dickson, Bedford, MA, USA) in 1xTBST for 1 h at room temperature and incubated overnight at 4 °C with the primary antibody of β-actin(Cell Signaling Technology, USA), P53(Cell Signaling Technology, USA), P21(Cell Signaling Technology, USA), Cyclin D1(Cell Signaling Technology, USA), Bax(Cell Signaling Technology, USA), Bcl-2(Cell Signaling Technology, USA), cleaved- PARP(Cell Signaling Technology, USA), PI3K(Cell Signaling Technology, USA), phospho-PI3K p85 (Tyr458)/p55 (Tyr199)(Cell Signaling Technology, USA), AKT(Cell Signaling Technology, USA), phospho-AKT (Ser473)(Cell Signaling Technology, USA), mTOR(Cell Signaling Technology, USA), phospho-mTOR (Ser2448)(Cell Signaling Technology, USA), p70 S6 Kinase(Cell Signaling Technology, USA), phospho-p70 S6 Kinase (Ser371)(Cell Signaling Technology, USA), 4E-BP1(Cell Signaling Technology, USA), phospho-4E-BP1 (Thr37/46)(Cell Signaling Technology, USA), ERK1/2(Cell Signaling Technology, USA), phospho-ERK1/2(Thr202/Tyr204)(Cell Signaling Technology, USA), p38 MAPK(Cell Signaling Technology, USA), phospho-p38 MAPK (Thr180/Tyr182)(Cell Signaling Technology, USA) at a 1:1000 dilution. The membranes were then incubated with fluorescent-based anti-mouse or anti-rabbit IgG secondary antibodies (Cell Signaling Technology, USA) at a 1:10,000 dilution for 1 h at room temperature. Observation and analysis of immunoreactive bands were performed using the Odyssey Infrared Imaging System (LI-COR biosciences, USA).

Tumor xenograft assay in nude mice

BALB/c nude mice (nu/nu, n = 24, 4 weeks old, 18.81±0.8 g) were purchased from Shanghai Laboratory Animal Center (Shanghai, China) and housed under specific pathogen-free(SPF) conditions in the animal care facilities of the Ninth People's Hospital, Shanghai Jiao Tong University School of Medicine. Animal welfare and experimental procedures were in compliance with the guide for the Care and Use of Laboratory Animals (the Ministry of Science and Technology of China, 2006) and the related ethical regulations of the hospital. The Laboratory Animal Care and Use Committees of the hospital approved all experimental procedures. In brief, a total of 2×10^6 Cal27 cells were washed three times in PBS and suspended in 50 μl DMEM mixed with 50μl Matrigel (Becton Dickson, Bedford, MA, USA) for a total volume of 100 μl per injection site. Subcutaneous injection was performed in the right side of the shoulder region. When the average tumor volume reached 100–150 mm [3], the mice were divided randomly into the control group and carrimycin group (n = 6 for each group). In the carrimyicn group, the mice were orally administered carrimycin solution (52 mg/kg) each day, while the control group were orally administered saline. The tumor volume and mice weight were measured every 2 days until the length of the tumor was greater than 1.5 cm, after which the mice were humanely sacrificed by euthanasia. The tumor volume (V) was calculated using tumor length (L) and width (W) as V=LxW^2/2. Xenograft samples were collected and analyzed by immunohistochemistry, western blot assay and TUNEL assay.

Immunohistochemistry

Four-micrometer-thick paraffin-embedded tumor sections were deparaffinized in xylene and rehydrated in decreasing concentration of ethanol. After heating in water bath at 100 °C with citrate buffer solution (pH=6.0) for 20 min to retrieve the antigen, sections were incubated in 3% H_2O_2 solution to abscise endogenous peroxidase activity and then in normal goat serum for 1 h. Next, the tumor sections were incubated with primary antibody against Ki-67 (1:200 dilution, Cell Signaling Technology, USA) overnight at 4 °C, followed by peroxidase-conjugated goat anti-rabbit antibody (Cell Signaling Technology, USA) for 1 h at room temperature. Finally, sections were developed in a substrate solution of DAB and counter-stained with hematoxylin and examined under light microscopy. The Ki-67 index was determined by the percentage of Ki-67-positive tumor cells in three random high-power microscopic fields.

TUNEL assay

For terminal deoxynucleotidyl transferase (TdT)-mediated nick-end labeling (TUNEL) staining, paraffin-embedded tumors from nude mice were assayed for DNA fragmentation using a TUNEL assay with the Fluorescein (FITC) Tunel Cell Apoptosis Detection Kit (Abcam, USA). The sections were rinsed in distilled water after deparaffinization and rehydration, and then incubated in 20 mg/L proteinase K (DAKO, Corporation, Carpinteria, CA, USA) at 37 °C for 20 min. After treating with 0.1% Triton, the sections were incubated in equilibration buffer and then in TdT enzyme solution in a humidified dark chamber at 37 °C for 2 h. Cell nucleus were stained by DAPI for 10 min. Sections were visualized using fluorescence microscope (Leica Micro systems).

Statistical analyses

All the experiments were performed at least three times. Data are presented as mean $\pm$ SD. Student's t-test (unpaired, two-tailed) was used to assess the difference of independent samples. $P<0.05$ was considered statistically significant.

Results

Carrimycin inhibited cell proliferation, colony formation and migration ability of OSCC cells

To evaluate the effect of carrimycin on OSCC cells *in vitro*, CCK8 assay, colony formation and wound healing assay were performed. The
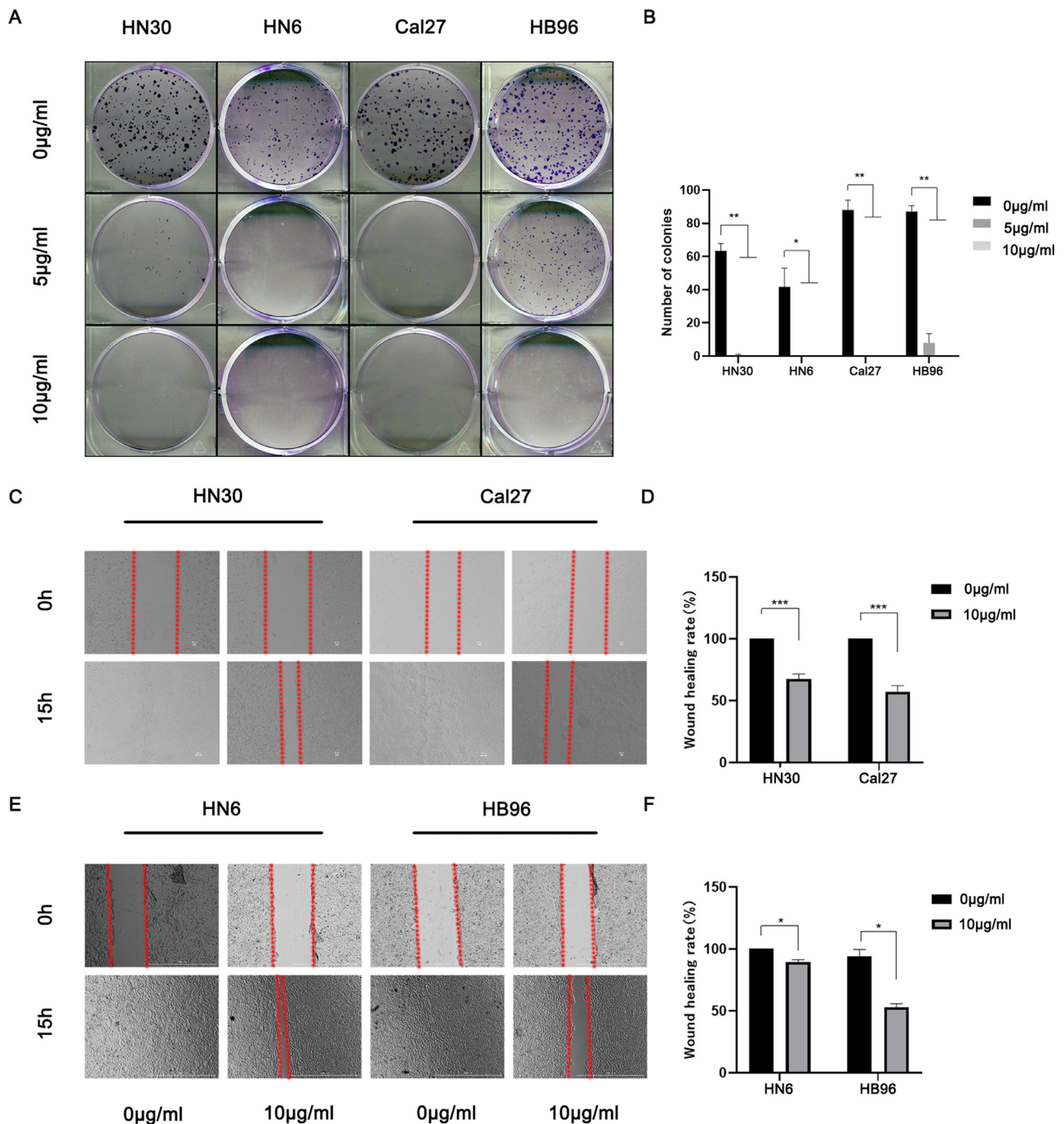
Fig. 2. Carrimycin inhibited colony formation and migration abilities of OSCC cells. (A,B) colony formation ability of HN30, HN6, Cal27 and HB96 cells was inhibited after treating with gradient concentration of carrimycin for 14 days. (C-F) Carrimycin decelerated the wound-healing rate of treated cells. All experiments were performed three times. $^{*}p < 0.05$, $^{**}p < 0.01$, $^{***}p < 0.001$.

growth of HN30, HN6, Cal27 and HB96 cells treated with carrimycin was inhibited in a time and dose dependent manner, and the IC50 (48 h) was shown for further assays (Fig. 1B–D). As shown in Fig. 2A and B, carrimycin could effectively suppress the colony formation capacity of OSCC cells. In addition, compared with the negative control, wound healing assay revealed a significant migration inhibition of OSCC cells after treating with 10 μg/ml carrimycin for 15h (Fig. 2C–F).

Carrimycin induced cell cycle arrest in G0/G1 phase

Flow cytometry was used to assess whether carrimycin could induce cell cycle arrest. After treating with 10 μg/ml carrimycin for 24 h, the proportion of G0/G1 phase was significantly increased while that of G2 phase decreased. The proportion of S phase was found to reduce in the HN6, Cal27 and HB96 cells, but no significant difference was observed in the HN30 cells (Fig. 3A and B). Western blot showed the up-regulation of P53 and P21, and the down-regulation of Cyclin D1, which was consistent with flow cytometry results (Fig. 3C and D). These results suggested that carrimycin could induce G0/G1 phase arrest in OSCC cells.

Carrimycin promoted cell apoptosis in OSCC cells

Annexin-V and PI double staining was used to mark apoptosis cells. As detected by flow cytometry, the apoptosis rate of OSCC cells was
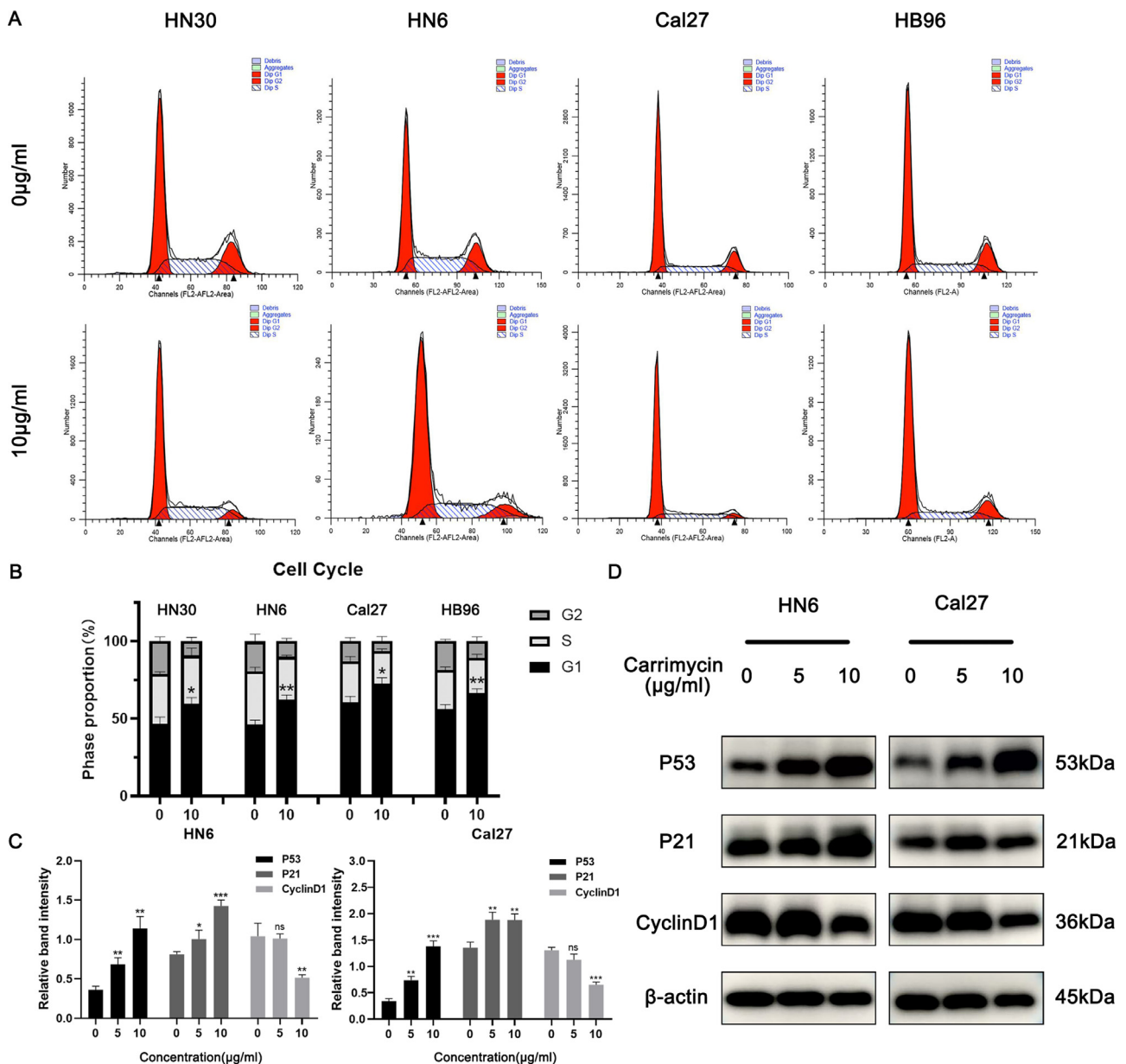
Fig. 3. Carrimycin induced cell cycle arrest in G0/G1 phase in OSCC cells. HN30, HN6, Cal27 and HB96 cells were hungered in FBS-free DMEM for 12 h, followed by treating with carrimycin at a concentration of 10 μg/ml and 0 μg/ml for 24 h. After staining with PI, cell cycle was assessed by flow cytometry. The expression of cell cycle-related proteins was detected by western blot. (A,B) the proportion of G0/G1 phase was significantly increased while that of G2 phase decreased. (C,D) The level of P53 and P21 was up-regulated after treating with gradient concentration of carrimycin (0, 5, 10 μg/ml) for 24 h, while that of CyclinD1 was down-regulated. β-actin was used as a loading control. All experiments were performed three times. ns $p > 0.05$, $^*p < 0.05$, $^{**}p < 0.01$, $^{***}p < 0.001$.

promoted with the increase of carrimycin concentration (Fig. 4A). In accordance with flow cytometry results, western blot showed the down-regulation of Bcl-2 and up-regulation of Bax. As a key protein of cell apoptosis, PARP was markedly cleaved in a dose-dependent manner (Fig. 4B and C). These results demonstrated that carrimycin could promote apoptosis in OSCC cells.

Carrimycin suppressed tumor growth in vivo

Xenograft model was established by subcutaneously injecting Cal27 cells in nude mice. After treating with carrimycin by intragastric administration for 19 days, the tumor volume was significantly suppressed compared with the NS-treated group, while the mice weight had no significant decrease (Fig. 5A and B). Immunohistochemistry and TUNEL assays were conducted to evaluate the proliferation marker Ki-

67 and apoptosis of xenograft tumor. The results showed that the expression of Ki-67 was markedly decreased in the carrimycin-treated group (Fig. 5C and D), while the apoptosis was significantly enhanced (Fig. 5E and F). In western blot of protein lysates extracted from xenograft samples, carrimycin-treated group showed a significant decrease of p-PI3K, p-AKT, p-mTOR, p-ERK and p-p38 compared with NS-treated group(Fig. 5G and H). Taken together, these findings indicated that carrimyicn could suppress tumor growth in vivo.

Carrimycin inhibited the biological activity of OSCC cells through PI3K/AKT/mTOR and MAPK signaling pathways

To investigate whether carrimycin could affect these pathways, total and phosphorylation level of PI3K, AKT, mTOR, S6K, 4EBP1, ERK and p38 were detected. In the Cal27 cells, the expression level of total AKT,
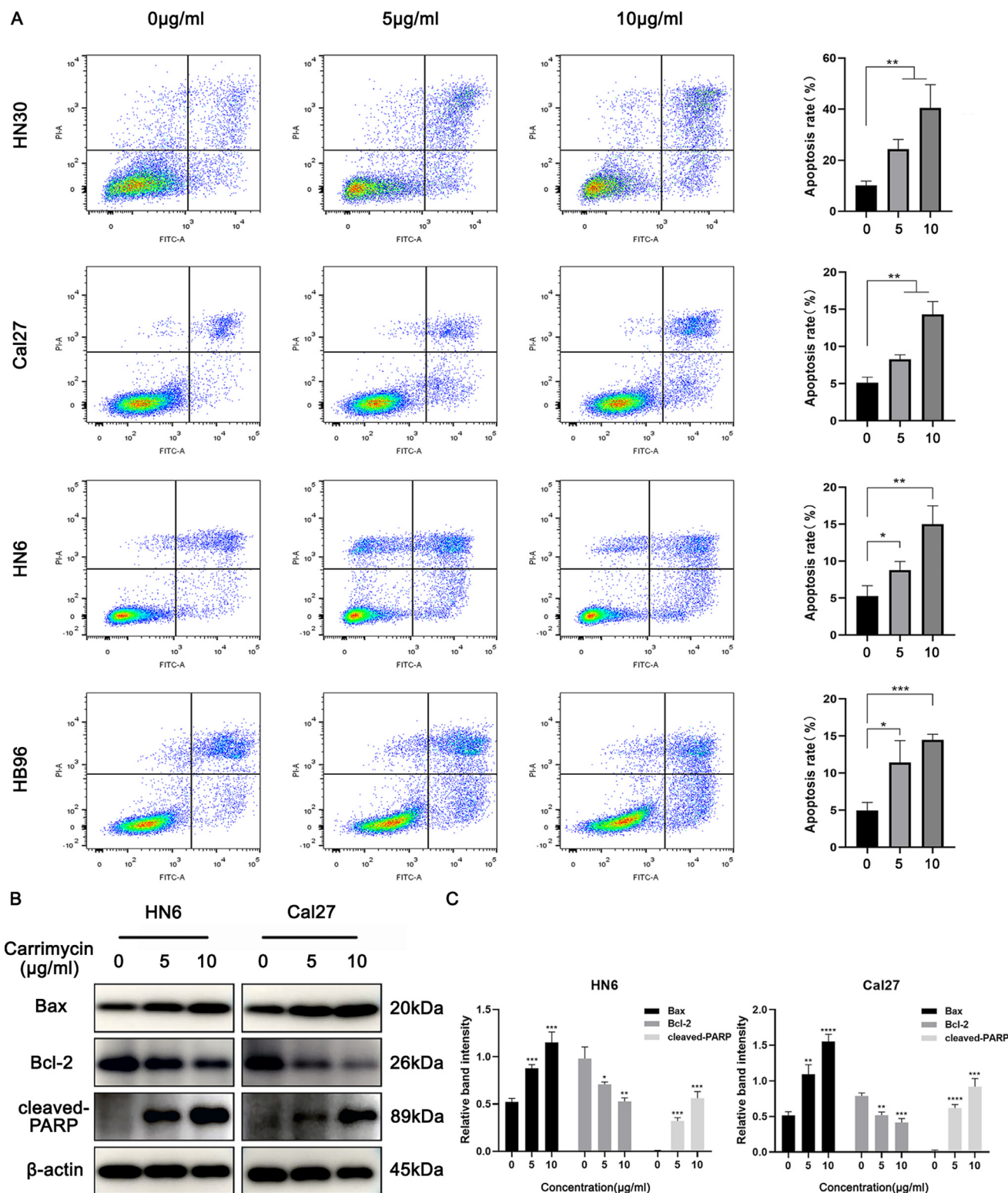
Fig. 4. Carrimycin promoted apoptosis of OSCC cells. HN30, HN6, Cal27 and HB96 cells were treated with carrimycin at a concentration gradient of 0 μg/ml, 5 μg/ml and 10 μg/ml for 24 h, and harvested for double-staining with the FITC-Annexin V Apoptosis Detection Kit. Cell apoptosis was assessed by flow cytometry. The expression of cell apoptosis-related proteins was detected by western blot. (A) the apoptosis rate of OSCC cells was promoted with the increase of carrimycin concentration. (B,C) western blot showed the down-regulation of Bcl-2 and up-regulation of Bax. As a key protein of cell apoptosis, PARP was markedly cleaved in a dose-dependant manner. β-actin was used as a loading control. All experiments were performed three times. $^*p < 0.05$, $^{**}p < 0.01$, $^{***}p < 0.001$, $^{****}p < 0.0001$.
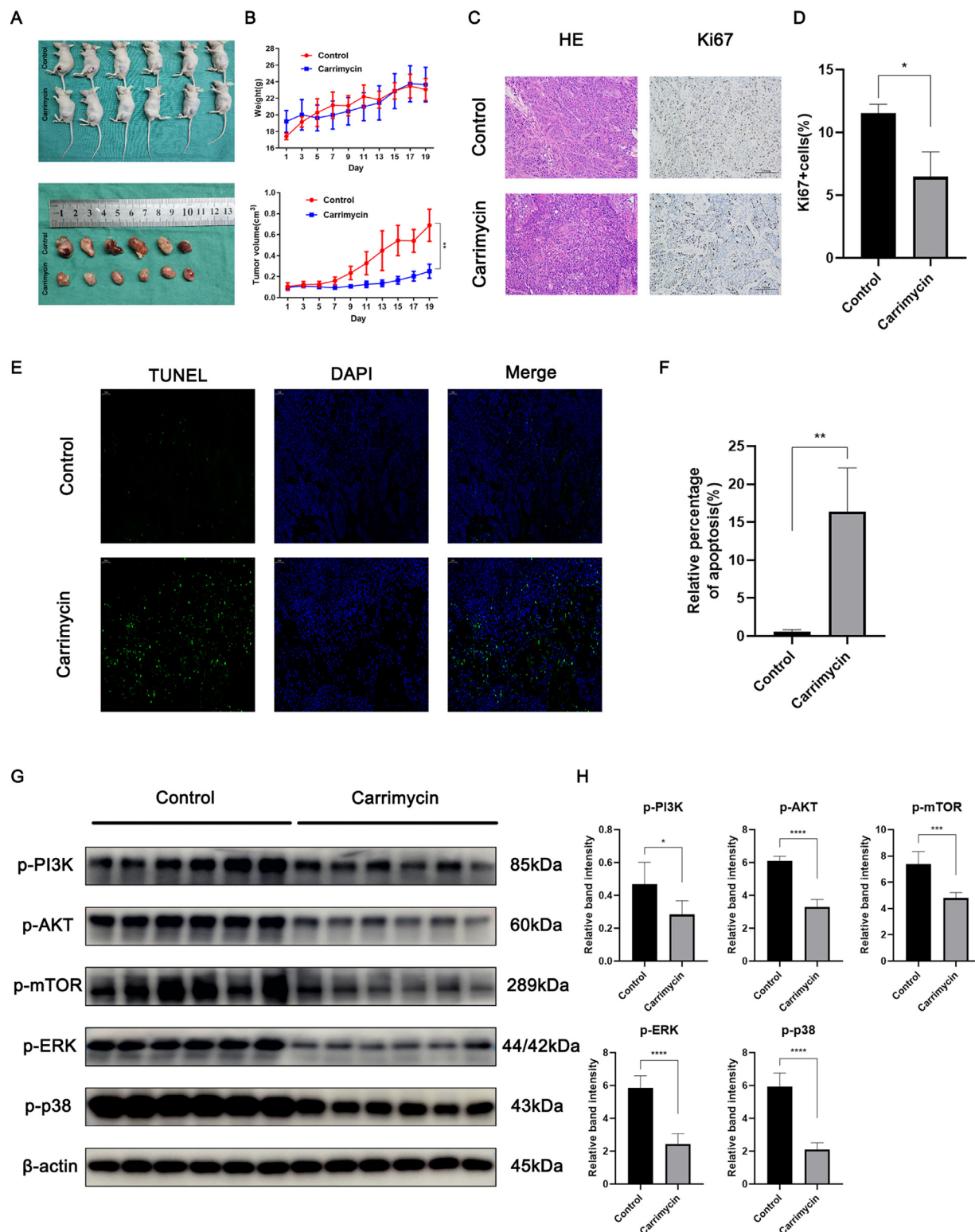
Fig. 5. Carrimyicin suppressed tumor growth in vivo. Xenograft model was established by subcutaneously injecting Cal27 cells in nude mice. After treating with carrimycin for 19 days, tumor volume and weight of nude mice were recorded. Immunohistochemistry, western blot and TUNEL assay were conducted. (A,B) the tumor volume was significantly suppressed compared with NS-treated group, while the mice weight had no significant decrease. (C,D) the expression of Ki67 was markedly decreased in carrimycin-treated group. (E,F) the cell apoptosis of xenograft tumors was significantly enhanced in carrimycin-treated group. (G,H) protein lysates extracted from xenograft samples of carrimycin-treated group showed a significant decrease of p-PI3K, p-AKT, p-mTOR, p-ERK and p-p38 compared with NS-treated group. All experiments were performed three times. $^{*}p < 0.05$, $^{**}p < 0.01$, $^{***}p < 0.001$, $^{****}p < 0.0001$.
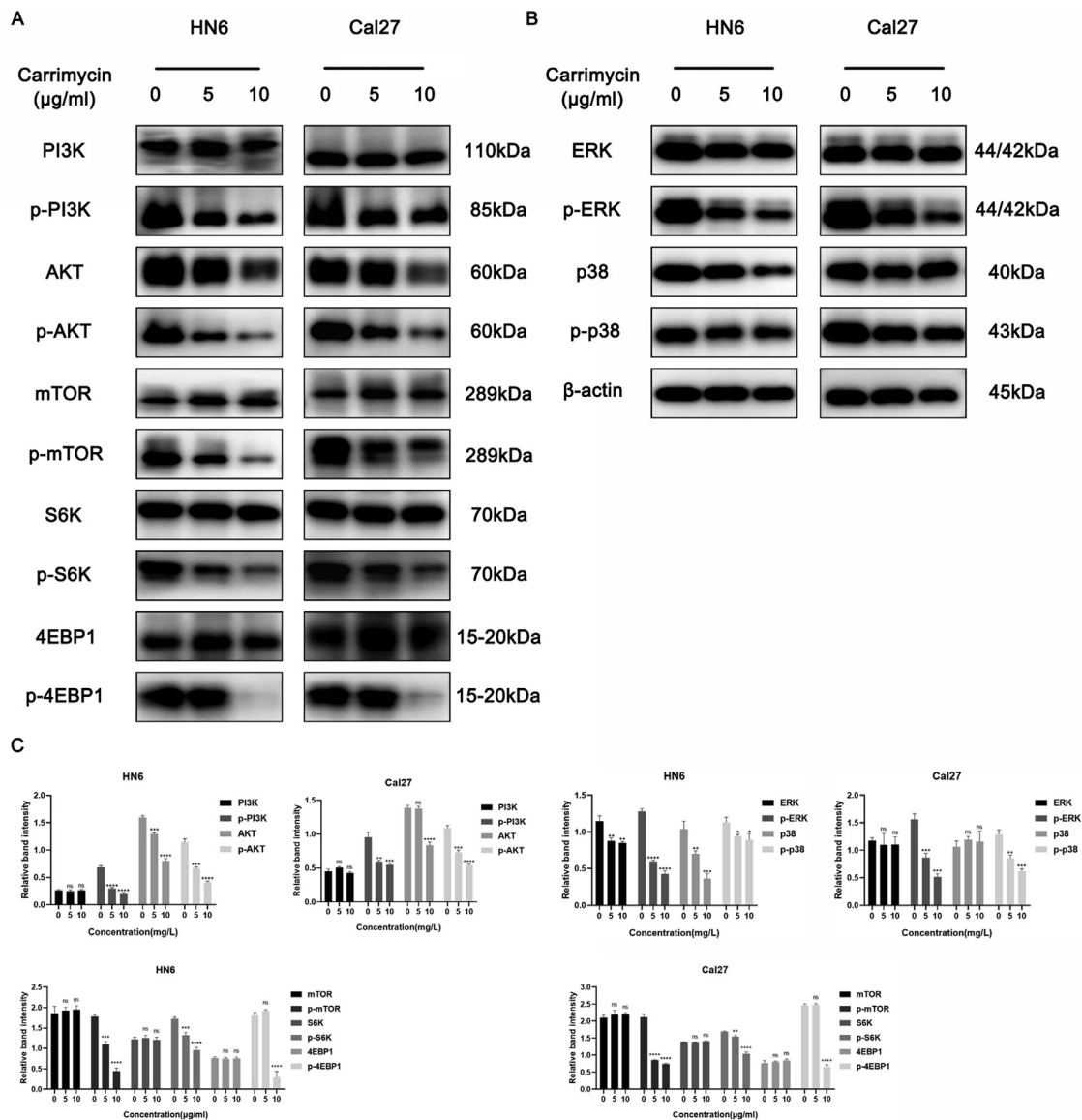
Fig. 6. The major proteins of PI3K/AKT/mTOR pathway and MAPK pathway were analyzed by western blot. (A-C) In the Cal27 cells, the expression level of total AKT, p-PI3K, p-AKT, p-mTOR, p-S6K, p-4EBP1, p-ERK and p-p38 significantly decreased after treating with carrimycin for 24 h. The same effect was observed in the HN6 cells. In addition, total ERK and total p38 were also down-regulated in the HN6 cells. All experiments were performed three times. ns $p > 0.05$, $^{*}p < 0.05$, $^{**}p < 0.01$, $^{***}p < 0.001$, $^{****}p < 0.0001$.

p-PI3K, p-AKT, p-mTOR, p-S6K, p-4EBP1, p-ERK and p-p38 significantly decreased after treating with carrimycin for 24 h. The same effect was observed in the HN6 cells. In addition, total ERK and total p38 were also down-regulated in the HN6 cells (Fig. 6A-C). Our western blot results could partially explain the inhibition effect of carrimycin on OSCC cells.

Discussion

In our study, we demonstrate that carrimycin can suppress the proliferation, colony formation and migration ability of OSCC cells, as well as induce cell cycle arrest and apoptosis. Animal experiment verify the same effect on xenograft tumors *in vivo*. Carrimycin-induced downregulation of PI3K/AKT/mTOR pathway and MAPK pathway may partially explain the potential mechanism of its inhibition effect.

Anti-tumor antibiotic drugs consist of anthracyclines, macrolides, glycopeptides, phenylalanine pyrrole, enediyne and quinoxaline, with high bioavailability and biosafety. Reviewing previous studies on antitumor mechanism of antibiotics, we summarize the mechanism as fol-

lows: destroying the double helix structure of DNA through free radical damage to interfere DNA replication, suppressing cell mitosis through inhibiting the depolymerization of tubulin, suppressing the key proteases of tumor cells to inhibit biological activities [9]. When it comes to macrolides antibiotics, immunosuppressor rapamycin inhibits tumor progression through targeting mammalian target of rapamycin (mTOR) [10]. Epothilone binds to microtubulin to suppress mitosis, and its analogs were reported to down-regulate the phosphorylation of AKT, ERK and p38 [11–13]. Another macrolides antibiotic tanespimycin(17-AAG), an inhibitor of HSP90, has also been proven to suppress p-ERK and p-AKT levels [14-17].

Since there's little study reporting the possible mechanism of carrimycin on tumor inhibition, based on the theories mentioned above, we hypothesize that carrimycin may exert its function through PI3K/AKT/mTOR pathway and MAPK pathway.

PI3K/AKT/mTOR signaling pathway is one of the major survival gateways of tumor cells, which serves as a cross point of multiple growth stimuli and regulates several cellular processes that contribute to the ini-

tiation and maintenance of cancer. Over-activation of PI3K/AKT/mTOR acts on its downstream substrates, leading to tumorigenesis through promotes tumor proliferation, migration and angiogenesis [18, 19]. Results in our study showed that carrimycin could markedly decrease the expression of p-PI3K, total AKT, p-AKT, p-mTOR, p-S6K, p-4EBP1 in a dose dependent manner in OSCC cell lines.

ERK and p38 belong to the mammalian family of mitogen-activated protein kinases (MAPKs) [20]. The MAPK pathways can be activated by diverse extracellular and intracellular stimuli. The main function of ERK signaling pathway is promoting cell growth and differentiation, and inhibition of p-ERK leads to tumor suppression, which is consistent with our study results. The function of p38 MAPK in cancer development is complex because of the wide range of cellular responses that it modulates [20, 21]. In our study, the phosphorylation of p38 was downregulated, suggesting that carrimycin mainly impaired the function of p38 as a tumor promoter.

When it comes to clinical translation, macrolide antibiotic rapamycin is limited in its application due to its poor water solubility, poor absorption capacity and low bioavailability [22]. There were several studies about its derivatives, such as everolimus, ridaforolimus and temsirolimus. Preclinical studies revealed a tumor inhibition effect of these drugs. However, the results of clinical trials were discouraging due to severe side effects and high toxicity. In a small sample phase II trial of everolimus, no objective responses were seen while three patients withdrew due to toxicity [23]. Clinical trials of macrolide antibiotics in combination with other drugs also showed poor therapeutic effect or severe side effects [24-27]. With good bioavailability and high biosafety confirmed by phase I clinical trial (data unpublished), carrimycin showed a promised future in clinical application.

However, it is worth noting that carrimycin is a compound whose main ingredients include isovalerylspiramycins I, II and III. The anti-tumor mechanism of each component is not clear yet and needs further investigation.

Conclusion

Our study verifies the anti-tumor effect of carrimycin on OSCC cells *in vitro* and *in vivo* for the first time, and reveals that carrimycin may exert its effect through PI3K/AKT/mTOR pathway and MAPK pathway.

Declaration of Competing Interest

None.

Acknowledgments

Funding

Availability of data and material

The datasets used or analysed during the current study are available from the corresponding author on reasonable request.

Author Contributions Statement

Conception and design: Si-yuan Liang, Tong-Chao Zhao, Wu-tong Ju, Dong-wang Zhu, Zhi-yuan Zhang, Lai-ping Zhong; experiment and analysis: Si-yuan Liang, Tong-Chao Zhao, Zhi-hang Zhou, Ying Liu, Yi-ran Tan, Dong-wang Zhu; drafting the manuscript for important intellectual content: Si-yuan Liang, Tong-Chao Zhao. All authors approved the final version of the manuscript prior to submission.

Supplementary materials

Supplementary material associated with this article can be found, in the online version, at doi:10.1016/j.tranon.2021.101074.

References

[1] 1 R.L. Siegel, K.D. Miller, A. Jemal, Cancer statistics, 2019, CA Cancer J. Clin. 69 (1) (2019) 7–34, doi:10.3322/caac.21551.

[2] 2 S.B. Chinn, J.N. Myers, Oral cavity carcinoma: current management, controversies, and future directions, J. Clin. Oncol. 33 (29) (2015) 3269–3276, doi:10.1200/JCO.2015.61.2929.

[3] 3 M. Cagel, E. Grotz, E. Bernabeu, M.A. Moretton, D.A. Chiappetta, Doxorubicin: nanotechnological overviews from bench to bedside, Drug Discov. Today 22 (2) (2017) 270–281, doi:10.1016/j.drudis.2016.11.005.

[4] 4 J. Chen, J. Stubbe, Bleomycins: towards better therapeutics, Nat. Rev. Cancer 5 (2) (2005) 102–112, doi:10.1038/nrc1547.

[5] 5 J.O. Eloy, R. Petrilli, D.L. Chesca, F.P. Saggioro, R.J. Lee, J.M. Marchetti, Anti-HER2 immunoliposomes for co-delivery of paclitaxel and rapamycin for breast cancer therapy, Eur. J. Pharm. Biopharm. 115 (2017) 159–167, doi:10.1016/j.ejpb.2017.02.020.

[6] 6 Z. Lu, X. Zhang, J. Dai, Y. Wang, W. He, Engineering of leucine-responsive regulatory protein improves spiramycin and bitespiramycin biosynthesis, Microb. Cell Fact. 18 (1) (2019) 38, doi:10.1186/s12934-019-1086-0.

[7] 7 L.P. Zhong, H.Y. Pan, X.J. Zhou, et al., Characteristics of a cancerous cell line, HIOEC-B(a)P-96, induced by benzo(a)pyrene from human immortalized oral epithelial cell line, Arch Oral Biol 53 (5) (May 2008) 443–452, doi:10.1016/j.archoralbio.2007.12.002.

[8] 8 D. Ye, X. Zhou, H. Pan, et al., Establishment and characterization of an HPV16 E6/E7-expressing oral squamous cell carcinoma cell line with enhanced tumorigenicity, Med. Oncol. 28 (4) (2011) 1331–1337, doi:10.1007/s12032-010-9558-4.

[9] 9 A.L. Demain, P. Vaishnav, Natural products for cancer chemotherapy, Microb. Biotechnol. 4 (6) (2011) 687–699, doi:10.1111/j.1751-7915.2010.00221.x.

[10] 10 K.G. Foster, D.C. Fingar, Mammalian target of rapamycin (mTOR): conducting the cellular signaling symphony, J. Biol. Chem. 285 (19) (2010,) 14071–14077, doi:10.1074/jbc.R109.094003.

[11] 11 M.J. Edelman, M. Shvartsbeyn, Epothilones in development for non–small-cell lung cancer: novel anti-tubulin agents with the potential to overcome taxane resistance, Clin. Lung Cancer 13 (3) (2012) 171–180, doi:10.1016/j.cllc.2011.02.005.

[12] 12 P. Giannakakou, R. Gussio, E. Nogales, et al., A common pharmacophore for epothilone and taxanes: molecular basis for drug resistance conferred by tubulin mutations in human cancer cells, Proc. Natl. Acad. Sci. U.S.A. 97 (6) (2000) 2904–2909, doi:10.1073/pnas.040546297.

[13] 13 Y.L. Li, J. Sun, X. Hu, et al., Epothilone B induces apoptosis and enhances apoptotic effects of ABT-737 on human cancer cells via PI3K/AKT/mTOR pathway, J. Cancer Res. Clin. Oncol. 142 (11) (2016) 2281–2289, doi:10.1007/s00432-016-2236-y.

[14] 14 C. Erlichman, Tanespimycin: the opportunities and challenges of targeting heat shock protein 90, Expert Opin. Investig. Drugs 18 (6) (2009) 861–868, doi:10.1517/13543780902953699.

[15] 15 S. Sato, N. Fujita, T. Tsuruo, Modulation of Akt kinase activity by binding to Hsp90, Proc. Natl. Acad. Sci. U.S.A. 97 (20) (2000) 10832–10837, doi:10.1073/pnas.170276797.

[16] 16 T.W. Schulte, M.V. Blagosklonny, C. Ingui, L. Neckers, Disruption of the Raf-1-Hsp90 molecular complex results in destabilization of Raf-1 and loss of Raf-1-Ras association, J. Biol. Chem. 270 (41) (1995) 24585–24588, doi:10.1074/jbc.270.41.24585.

[17] 17 F. Dou, L.D. Yuan, J.J. Zhu, Heat shock protein 90 indirectly regulates ERK activity by affecting Raf protein metabolism, Acta Biochim. Biophys. Sin. Shanghai 37 (7) (2005) 501–505, doi:10.1111/j.1745-7270.2005.00069.x.

[18] 18 J. LoPiccolo, G.M. Blumenthal, W.B. Bernstein, P.A. Dennis, Targeting the PI3K/Akt/mTOR pathway: effective combinations and clinical considerations, Drug Resist. Updates Rev. Comment. Antimicrob. Anticancer Chemother. 11 (1–2) (2008) 32–50, doi:10.1016/j.drup.2007.11.003.

[19] 19 I. Hers, E.E. Vincent, J.M. Tavare, Akt signalling in health and disease, Cell Signal 23 (10) (2011) 1515–1527, doi:10.1016/j.cellsig.2011.05.004.

[20] 20 E.K. Kim, E.J. Choi, Pathological roles of MAPK signaling pathways in human diseases, Biochim. Biophys. Acta 1802 (4) (2010) 396–405, doi:10.1016/j.bbadis.2009.12.009.

[21] 21 E.F. Wagner, A.R. Nebreda, Signal integration by JNK and p38 MAPK pathways in cancer development, Nat. Rev. Cancer 9 (8) (2009) 537–549, doi:10.1038/nrc2694.

[22] 22 L. Liu, J. Chen, X. Cai, Z. Yao, J. Huang, Progress in targeted therapeutic drugs for oral squamous cell carcinoma, Surg. Oncol. 31 (2019) 90–97, doi:10.1016/j.suronc.2019.09.001.

[23] 23 J.L. Geiger, J.E. Bauman, M.K. Gibson, et al., Phase II trial of everolimus in patients with previously treated recurrent or metastatic head and neck squamous cell carcinoma, Head Neck 38 (12) (2016) 1759–1764, doi:10.1002/hed.24501.

[24] 24 J.E. Bauman, H. Arias-Pulido, S.J. Lee, et al., A phase II study of temsirolimus and erlotinib in patients with recurrent and/or metastatic, platinum-refractory head and neck squamous cell carcinoma, Oral Oncol. 49 (5) (2013) 461–467, doi:10.1016/j.oraloncology.2012.12.016.

[25] 25 S.A. Piha-Paul, P.N. Munster, A. Hollebecque, et al., Results of a phase 1 trial combining ridaforolimus and MK-0752 in patients with advanced solid tumours, Eur. J. Cancer 51 (14) (2015) 1865–1873, doi:10.1016/j.ejca.2015.06.115.

[26] 26 E.E. Cohen, M.R. Sharma, L. Janisch, et al., A phase I study of sirolimus and bevacizumab in patients with advanced malignancies, Eur. J. Cancer 47 (10) (2011) 1484–1489, doi:10.1016/j.ejca.2011.02.017.

[27] 27 P.C. Barata, M. Cooney, P. Mendiratta, R. Gupta, R. Dreicer, J.A. Garcia, Phase I/II study evaluating the safety and clinical efficacy of temsirolimus and bevacizumab in patients with chemotherapy refractory metastatic castration-resistant prostate cancer, Invest. New Drugs 37 (2) (2019) 331–337, doi:10.1007/s10637-018-0687-5.